UNIVERSITY POLITEHNICA OF BUCHAREST
DOCTORAL SCHOOL OF APPLIED CHEMISTRY AND MATERIALS SCIENCE

PhD THESIS

§ SUMMARY §

MULTIFUNCTIONAL BIONANOSTRUCTURED MATERIALS

Author: Eng. Mariana Oana Mihaela FUFĂ (GHERASIM)

Doctoral supervisor: Prof. PhD Eng. Ecaterina ANDRONESCU

Doctoral guiding committee: Assoc. Prof. PhD Eng. Alexandru Mihai GRUMEZESCU

Prof. PhD Eng. Anton FICAI

Prof. PhD Chem. Ovidiu Cristian OPREA

Doctoral thesis defense committee

President	Prof. PhD Eng. Adelina Carmen IANCULESCU	from	University Politehnica of Bucharest
Doctoral supervisor	Prof. PhD Eng. Ecaterina ANDRONESCU	from	University Politehnica of Bucharest
Member	Assoc. Prof. PhD Eng. Alexandru Mihai GRUMEZESCU	from	University Politehnica of Bucharest
Member	Prof. PhD Biol. Carmen Mariana CHIFIRIUC	from	University of Bucharest
Member	Prof. PhD MD Laurențiu MOGOANTĂ	from	University of Medicine and Pharmacy of Craiova

Bucharest

2021

Table of Contents

Keywords:

- ✓ metallic and metal oxide nanoparticles
- ✓ hybrid biopolymeric microspheres
- ✓ bioactive nanostructured coatings
- ✓ anti-infective therapy
- ✓ tissue engineering

Critical literature study

The current challenges of conventional pharmaceutical strategies result from various treatment-related and patient-related shortcomings, such as (i) non-specificity or non-selectivity of the selected therapeutic agent, (ii) inadequate or incorrect treatment administration, and (iii) pharmacological-derived side effects [1,2]. In order to overcome such unwanted events, tremendous interdisciplinary knowledge has been oriented towards the nanotechnology-based development of novel and enhanced pharmaceuticals.

An alarming phenomenon of current healthcare practice is the occurrence and severity of infection-related complications caused by drug-resistant and biofilm-embedded microorganisms. With the aim to combat such pathogens and to limit the life-threatening complications, worldwide researches focused on the investigation of antibacterial resistance mechanisms, as well as on the development and optimization of unconventional and effective antibacterial strategies.

Nanosized and nanostructured biomaterials represent a feasible choice for the fabrication of new platforms and medical devices with improved antimicrobial efficacy. Given their (i) intrinsic biocompatibility, (ii) reduced toxic effects in healthy cells, (iii) biocide or biostatic effects against pathogenic cells, (iv) remarkable possibilities for surface derivatization and functionalization, and (v) genuine size-related physicochemical features (optical, electrical and magnetic properties governed by quantum effects), inorganic nanoparticles are promising candidates for the fabrication of performance-enhanced anti-infective formulations [3,4].

Among zero-dimensional nanomaterials, silver nanoparticles (AgNPs) and magnetite nanoparticles (Fe_3O_4 NPs) represent the most explored and successful candidates for modern biomedical applications, with formidable results being reported in pharmaceutical sciences, cosmetic products, wound dressings, tissue engineering and regenerative medicine, biodetection and biomedical imaging, anti-infective therapy and cancer treatment. The impressive potential of AgNPs and Fe_3O_4 NPs in biomedicine relies on their intrinsic peculiarities, such as excellent antimicrobial efficiency and unique optical properties, surface versatility and tunable magnetic behavior, respectively.

Owing to their attractive features, including (i) bioavailability, (ii) compositional and structural versatility, (iii) facile processability, (iv) tunable physicochemical, mechanical and thermal properties, (v) adjustable solubility, dissolution and degradability, (vi) circumstantial triggered biodegradability and non-toxic metabolites, (vii) remarkable reactivity-related

derivatization and functionalization potential, (viii) biocompatibility, non-toxicity and non-immunogenicity, (ix) intrinsic biological activity (antioxidant, anti-inflammatory, antimicrobial, anti-tumor, analgesic, hemostatic effects), and (x) in particular, specialized institutional approval, biopolymers are promising candidates for modern antimicrobial formulations [5-7].

Natural-derived (polysaccharides, polyhydroxyalkanoates) and synthetic (aliphatic polyesters) polymers are essential elements for the development of new micro-/nanostructured pharmacotherapeutics. The excellent biofunctionality revealed during preclinical studies demonstrates the effective use of biopolymer formulations in anti-infective and anti-tumor therapy, detection and diagnosis, gene therapy and regenerative medicine.

The clinical outcomes of implantable medical devices (IMDs) are strongly related to the physicochemical and biological properties of their surface [8-10]. Surface modification by means of laser-processed bioactive coatings was revealed as an auspicious and attractive unconventional strategy to overcome the confined functionality of conventional IMDs. In particular, thin films obtained by matrix-assisted pulsed laser evaporation represent attractive and promising candidates for biomedical applications, including antimicrobial therapy, biomolecular detection, and tissue regeneration and functional restoration.

Titanium (Ti) and its alloys represent suitable candidates for the fabrication of implantable devices intended to restore and replace severely damaged hard tissues or bone losses. In order to exceed the bioinertness and limited bioactivity of metallic biomaterials and to mediate the osseointegration of Ti-based implants, extensive efforts were oriented towards their surface modification with osteoconductive or osteoinductive coatings. Surface modification by calcium phosphates (CaPs) coatings obtained by laser processing represents a suitable choice to boost the integration of metallic implants and improve their overall biofunctionality [11,12]. CaPs ceramics possess an important role in hard tissue engineering applications owing to their specific characteristics, which include (i) biomimetic composition, (ii) suitable mechanical properties, (iii) superior chemical stability, (iv) tunable microstructure and degradability, and (v) excellent biocompatibility [13,14].

Original contributions

Purpose and specific objectives of the research activity

The research topic of the doctoral thesis is part of the global strategies regarding the development of multifunctional and bioactive formulations with therapeutic efficacy, addressing the following areas of interest: (i) enhancing the pharmacological effects of antimicrobial and anti-inflammatory biosubstances by using biopolymer systems; (ii) preventing and limiting the microbial contamination and colonization phenomena of biomedical materials and devices by their surface modification; and (iii) modulating periprosthetic infections and the regenerative ability of metallic implants by means of nanostructured coatings loaded with growth factors.

The main purpose of the research activity was to develop bioactive nanostructured platforms for anti-infective therapy and tissue engineering applications. In this respect, we aimed the synthesis, optimization and (micro)biological evaluation of nanosized biomaterials (nanoparticles conjugated with bioactive principles, biopolymer thin films) and nanostructured biomaterials (biopolymer microspheres loaded with therapeutic agents, composite coatings).

Specific objectives of the research activity included: (i) the synthesis, characterization and evaluation of inorganic nanosystems functionalized with phytochemicals or synthetic drugs; (ii) the obtaining, optimization and assessment of micro-/nanostructured systems (biopolymeric spheres embedded with therapeutic agents and/or functionalized nanoparticles); (iii) the fabrication of nanostructured biopolymer films for preventing and limiting the microbial contamination and colonization of biomedical surfaces, using the Matrix–Assisted Pulsed Laser Evaporation (MAPLE) technique; and (iv) the synthesis, optimization and evaluation of coatings loaded with bioactive substances and nanostructured biomimetic coatings modified with biomolecules (growth factors).

Results and discussions

1. Pharmacotherapeutic bioactive formulations

1.1. Hybrid systems based on poly(3-hydroxybutyrate-co-3-hydroxyvalerate), chitosan and antibiotics

Composite polymeric particles based on poly(3-hydroxybutyrate-co-3-hydroxyvalerate) and chitosan, P(3HB-3HV)-CS, were proposed as biocompatible and biodegradable delivery systems for bioproduced antibiotics: bacitracin (Bac), neomycin (Neo) and kanamycin (Kan) [15].

As revealed by the SEM micrographs, aggregates of spherical particles were obtained, regardless of the composition (Figure 1.1.1). Similar dimensions (~600 nm) were noticed in the case of simple and Bac-loaded P(3HB-3HV)-CS. Particle sizes of ~400 nm and ~1 μm were evidenced in the case of P(3HB-3HV)-CS-Neo and P(3HB-3HV)-CS-Kan systems, respectively.

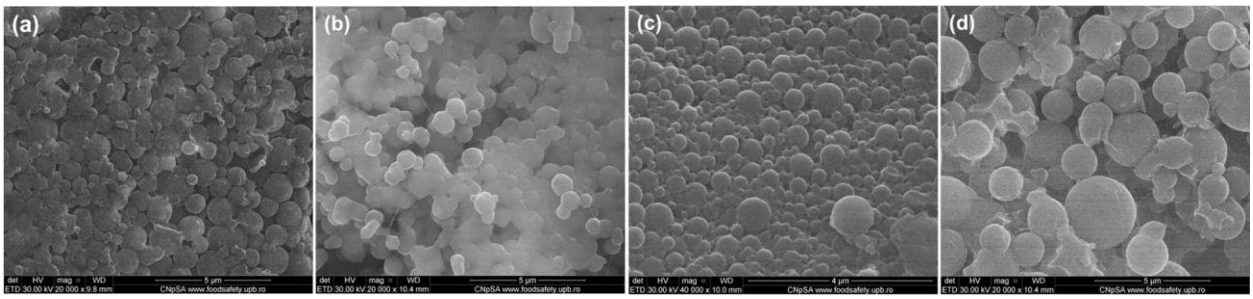

Figure 1.1.1: SEM micrographs of P(3HB-3HV)-CS (a), P(3HB-3HV)-CS-Bac (b), P(3HB-3HV)-Neo (c) and P(3HB-3HV)-CS-Kan (d) spheres

Individual and overlapped IR spectra were recorded from different points for all synthesized spheres. The presence of P(3HB-3HV) was confirmed through the following absorption bands: ~1720 cm^{-1} (strong stretching vibrations of C=O ester group, particularly asscociated with the crystalline phase), ~1378 cm^{-1} (symmetric expansion of $–CH_3$), ~1276 cm^{-1} (C–H stretching), ~1054 cm^{-1} (C–O–C stretching) and ~978 cm^{-1} (C–C stretching) [16,17]. The zoomed in IR spectra evidenced the presence of specific CS maxima at ~1671 cm^{-1} (amide II), ~1650 cm^{-1} and ~1635 cm^{-1} (amide I doublet) and ~1557 cm^{-1} (C–O skeletal vibrations) [18,19].

Growth inhibition results showed that the obtained spheres could enhance the effects of antibiotics (ATB) against the selected bacteria. The diameters of growth inhibition were higher in the case of P(3HB-3HV)-CS-Neo and P(3HB-3HV)-CS-Kan spheres, as compared to the plain antibiotic controls (Kan and Neo). The strongest antimicrobial effect was observed for the Gram-negative species. P(3HB-3HV)-CS-Bac spheres proved their potentiating effects on the bacitracin action against Gram-positive bacteria.

The CCD-1070Sk cell line was selected for assessing the cytotoxic potential of proposed antibiotic-loaded composites. The metabolic activity of dermal fibroblasts presented no significant differences of the cellular viability, and the ability of ATB-loaded systems to sustain and promote the proliferation of dermal fibroblasts – as highlighted by the statistically significant increase ($p < 0.0001$) of cellular viability after 7 days. Also, the antibiotic delivery platforms did not alter the structural integrity of the cellular membrane (evidenced by quantifying the level of LDH released in the culture medium). Moreover, no differences between the assembly of actin

filaments of untreated fibroblasts and treated cells were noticed. The human dermal fibroblasts uniformly spread on the culture dish under all investigated experimental conditions, while maintaining their typical spindle-like morphology and ability to form strong intercellular compact networks. The basal level of H_2O_2 detected in the untreated CCD-1070Sk cultures was similar to the H_2O_2 levels detected in the fibroblasts cultures exposed to simple and ATB-loaded spheres treatment at both experimental time points, showing that the composites did not induce oxidative stress (Figure 1.1.2a).

Complementary assays performed on endotoxin-activated RAW 264.7 murine macrophages evidenced the ability of Bac-/Neo-/Kan-loaded spheres to augment the NO production, depending on the testing time and the presence of antibiotics (Figure 1.1.2b). Both LPS activation and exposure to simple and antibiotic-loaded spheres did not stimulate the production of IL-10, IFN-γ and IL-12p70 in RAW 264.7 cell cultures. The spheres treatment affected the LPS-activated profile of IL-6 and TNF-α proinflammatory cytokines in an antibiotic-dependent manner. The expression of IL-6 was significantly increased ($p < 0.05$) only in LPS-activated macrophages treated with P(3HB-3HV)-CS-Kan spheres. An increase in TNF-α expression was identified in RAW 264.7 activated cells exposed to P(3HB-3HV)-CS-Neo and P(3HB-3HV)-CS-Kan spheres.

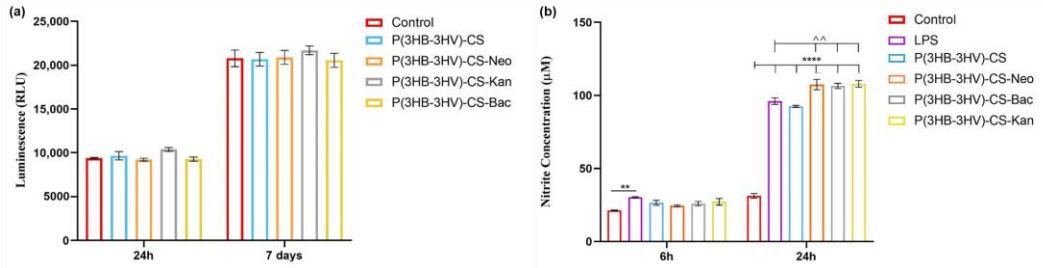

Figure 1.1.2: Graphic representation of the H_2O_2 levels in human dermal fibroblasts cell cultures exposed for 24h and 7 days at simple and Bac-/Neo-/Kan-loaded P(3HB-3HV)-CS spheres treatment (a);
Graphic representation of the nitrite levels as a measure of NO release in LPS-activated RAW 264.7 macrophages cell cultures exposed for 6h and 24h to simple and Bac-/Neo-/Kan-loaded P(3HB-3HV)-CS spheres treatment (b)
(** $p \leq 0.01$ LPS *vs.* control; ^^ $p \leq 0.01$ sample *vs.* LPS; **** $p \leq 0.0001$ sample *vs.* untreated control)

P(3HB-3HV)-CS biopolymeric spheres proved significant potentiating effects on common antibiotics, being effective against both Gram-positive and Gram-negative species. The antibiotic-loaded composites showed absent or reduced proinflammatory effects on macrophages and proved beneficial for long-term proliferation of human dermal fibroblasts, without microstructural alterations.

1.2. Hybrid systems based on poly(lactide-co-glycolide), chitosan and magnetite nanoparticles modified with non-steroidal anti-inflammatory drug

Herein, we reported the synthesis and evaluation of poly(lactide-co-glycolide) spheres containing different amounts of magnetite nanoparticles and ibuprofen (PLGA-Fe_3O_4-IBUP), but also chitosan (PLGA-CS-Fe_3O_4-IBUP), to be considered as drug delivery systems [20].

The SEM analysis of PLGA-Fe_3O_4-IBUP systems – obtained by adding 10, 20, and 50 mg of magnetite nanopowder (IBUP10, IBUP20 and IBUP50, respectively) – evidenced the formation of well-defined and individual particles with spherical morphology and comparable dimensions. A prevalent smooth surface and a narrower dimensional distribution were observed in the case of IBUP10 and IBUP20 samples, as a consequence of the complete and uniform embedding of magnetic NPs within the polymeric matrix. By contrast, IBUP50 microspheres possessed rather textured surface and had more heterogenic dimensions. The IR results confirmed the synthesis of nanostructured composite microspheres.

The evaluation of PLGA-Fe_3O_4-IBUP microspheres under biologically simulated conditions evidenced minimal compositional changes and morphological alterations in the particular case of IBUP10 systems, after three weeks of dynamic testing.

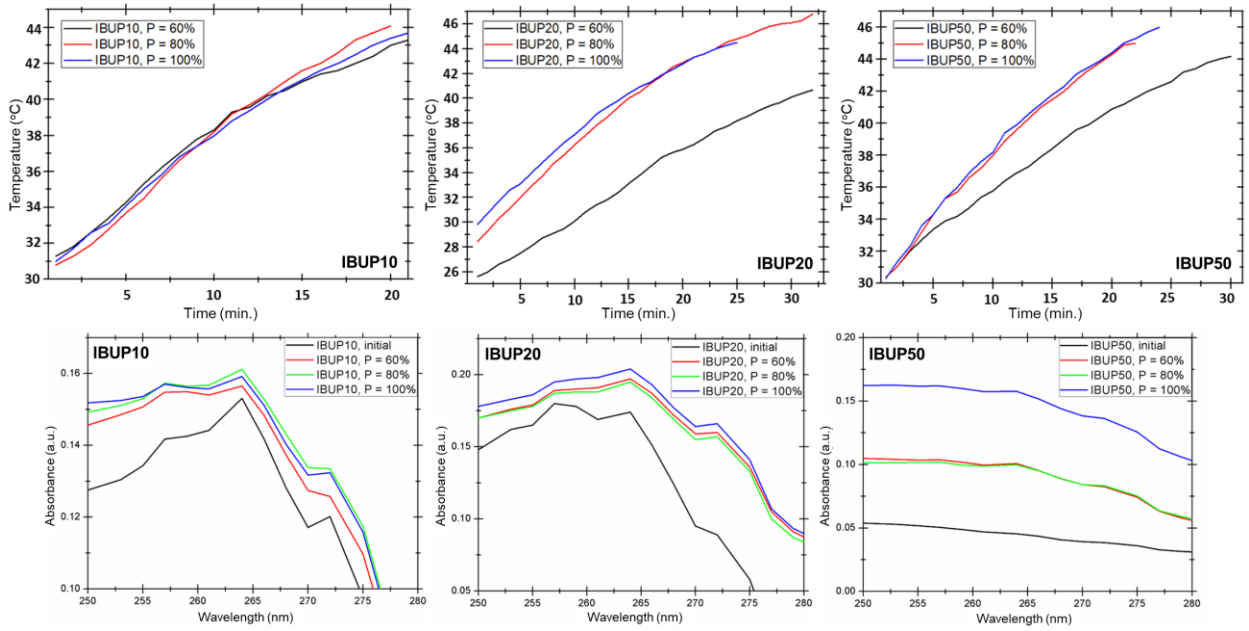

Figure 1.2.1: Temperature evolution of PLGA-Fe_3O_4-IBUP biopolymeric spheres in the presence of different magnetic fields (top); UV-Vis spectra of PLGA-Fe_3O_4-IBUP systems resulted after hyperthermia tests (down)

We further assessed the potential use of PLGA-Fe_3O_4-IBUP microspheres in hyperthermia applications and aimed to identify the suitable composition that provided maximal effect for future safe investigations. A particular case was noticed for the IBUP10 nanostructured microspheres, in which the heating effect was comparable, regardless of the power of external magnetic field (Figure 1.2.1, top). The most prominent drug release effect was assigned to the IBUP20 systems exposed to 100% magnetic field strength, followed by the IBUP10 systems exposed to the radiofrequency magnetic field with the lowest strength (1.2 kW, representing 60% of the maximum output power) (Figure 1.2.2, down).

The biological assessment of thin films of nanomagnetite-embedded biopolymeric spheres of drug-free PLGA (S), IBUP-loaded PLGA (IBUP10), or IBUP-loaded PLGA-CS (IBUP10 CS) revealed the beneficial effects of all nanostructured materials on the viability, adhesion and normal growth of human macrophages. The effects were enhanced in the case of IBUP10 and IBUP10CS.

Microbial planktonic cultures were significantly inhibited in the presence of coatings containing either IBUP or CS and IBUP. The addition of CS within the biopolymeric spheres resulted in the most prominent inhibitory effects against planktonic growth, independent of the microbial strain.

Complementary results demonstrated that biofilm development was especially inhibited by the CS-containing composites (Figure 1.2.2). The most prominent inhibitory effects were exhibited against the contamination and colonization stages of *S. aureus*. However, coatings containing plain IBUP-encapsulated PLGA nanostructured microspheres also exhibited slight biofilm inhibition ability, this effect being especially manifested in the case of *P. aeruginosa*.

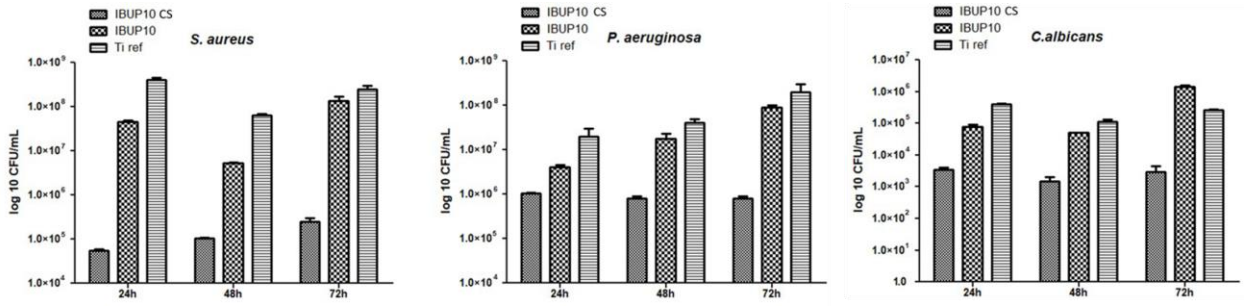

Figure 1.2.2: Dynamic biofilm formation ability of tested microbial species in the presence of composite biopolymeric spheres coatings

The composite biopolymeric spheres possess multifunctional features, since their subsequent evaluation may include platforms for controlled and triggered therapy of severe diseases, but also coatings for implantable devices intended for chronic condition management.

1.3. Coatings based on poly(lactide-co-glycolide) and non-steroidal anti-inflammatory drug

In this study, we evaluated the ability of poly(lactide-co-glycolide) coatings to act as active matrices for the release of ibuprofen under biomimetic simulated conditions, but also their complex cellular response [21].

Following the biologically simulated testing of PLGA/IBUP coatings, performed under dynamic conditions, the slow degradation of the polymer matrix (relative mass loss between ~7.89% and ~16.75%, after 2 and 30 days of dynamic studies, respectively) and the progressive drug release (cumulative release of IBUP between ~90 µg/mL and ~250 µg/mL) were evidenced. Reversible swelling phenomena of polymeric coatings occurred in the first two weeks of testing, followed by their irreversible degradation and chemical alteration after one month. The SBF-mediated hydrolysis of PLGA matrix was evidenced by a significant shift of carbonyl moiety (between 1750–1710 cm^{-1}) originating either from PLGA (until 15th day of testing) or from LA and GA units (20 and 30 days of testing) (Figure 1.3.1).

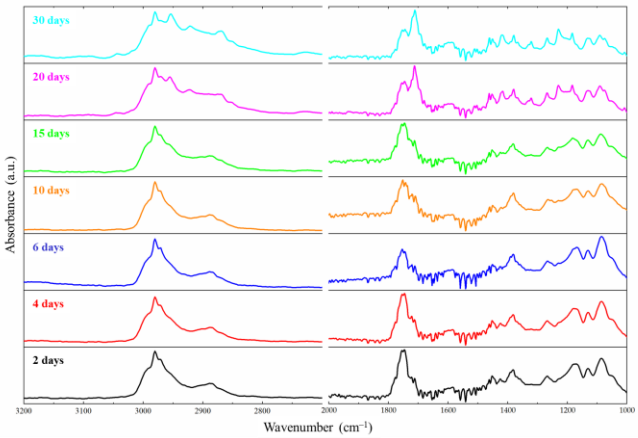

Figura 1.3.1: ATR-FTIR spectra of PLGA/IBUP coatings during biologically simulated dynamic testing

In this work, THP-1 cells differentiated to macrophages were used to investigate the interaction with PLGA/IBUP coatings. The quantitative data revealed that all PLGA-based coatings induced a significant increase in cell viability ($p < 0.001$) at 3 days, compared to the 1-day time point. The beneficial effects of proposed coatings on cell adhesion, spreading and morphology were complementary determined by microscopic examination (Figure 1.3.2, top), confirming the highly biocompatible behavior of PLGA-based materials with respect to human macrophages.

The ability of PLGA/IBUP coatings to sustain the survival and promote the proliferation of human fibroblasts was demonstrated by qualitative (viable cells visualization and counting) and

quantitative (metabolic activity evaluation, Figure 1.3.2a) assays. The cellular studies performed to investigate the adhesion and cellular morphology confirmed the highly cytocompatible feature of PLGA/IBUP coatings with respect to human fibroblasts. Moreover, PLGA-based materials determined a time-dependent increase in collagen synthesis by fibroblasts (Figure 1.3.2b).

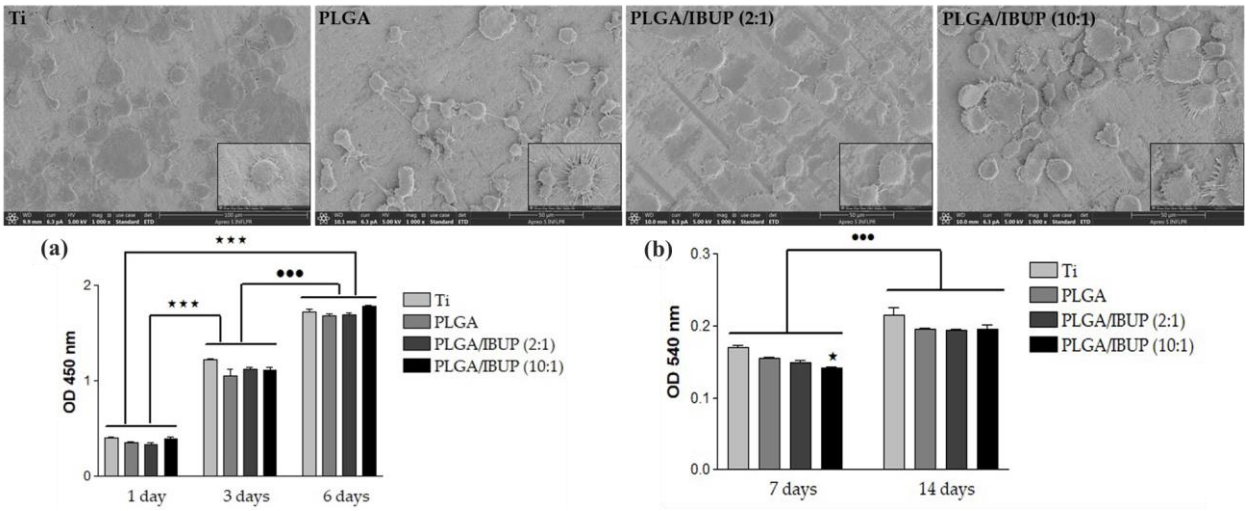

Figure 1.3.2: Morphological features of human macrophages on PLGA-based coatings after 3 days, evidenced by SEM (top); Viability and proliferation of human fibroblasts grown in contact with PLGA-based coatings for 1, 3 and 6 days (a) (★★★$p < 0.001$ *vs.* 1 day; ••• $p < 0.001$ *vs.* 3 days); Collagen synthesis of human fibroblasts grown on PLGA-based coatings for 7 and 14 days (b) (★ $p < 0.05$ *vs.* Ti; ••• $p < 0.001$ *vs.* 7-days time point)

Cell-to-substrate adhesion and morphology of KERTr cells grown on PLGA/IBUP coatings were evaluated by concomitant visualization of green-labeled vinculin and red-labeled actin (Figure 1.3.4). All cells exhibited typical polygonal morphology, enhanced focal adhesions and well-defined cellular cortex after 24h of incubation, regardless of the substrate.

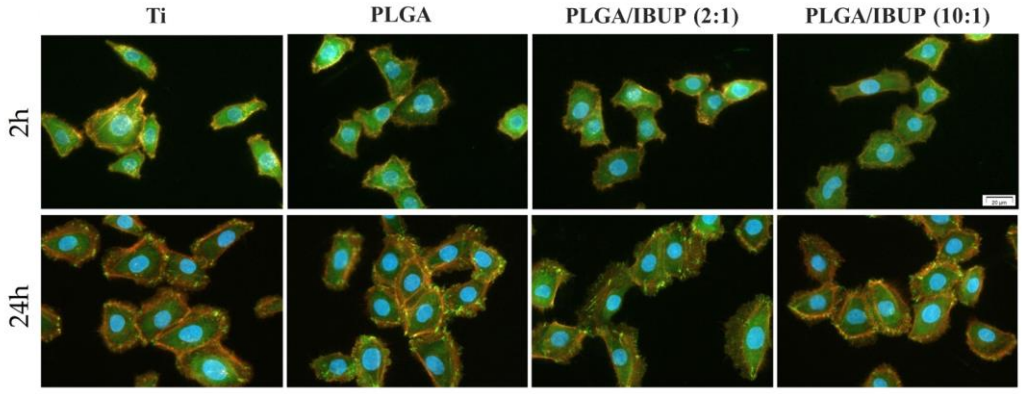

Figure 1.3.3: Adhesion and morphology of human keratinocytes on PLGA-based coatings after 2h and 24h, evidenced by FM showing vinculin protein (green), actin filaments (red) and nuclei (blue)

Complementary, the ability of KERTr cells to adapt to surface features and their potential to proliferate were evidenced by SEM investigation, while the beneficial role of PLGA/IBUP

coatings on supporting the viability and encouraging the proliferation of keratinocytes were demonstrated by FM and metabolic activity studies.

The composite materials demonstrated gradual degradation and long-term drug release under biologically simulated dynamic conditions. Excellent cytocompatibility was evidenced on human-derived macrophages, fibroblasts and keratinocytes, highlighting the promising potential of PLGA/IBUP coatings to be used for surface modification of medical devices, like metallic implants and wound dressings.

2. Antimicrobial nanostructured surfaces

2.1. Thin films based on polylactide and silver nanoparticles

Nanostructured materials based on polylactic acid (PLA) and silver nanoparticles (AgNPs) were proposed as bioactive coatings able to prevent the formation of microbial biofilms on biomedical surfaces [22].

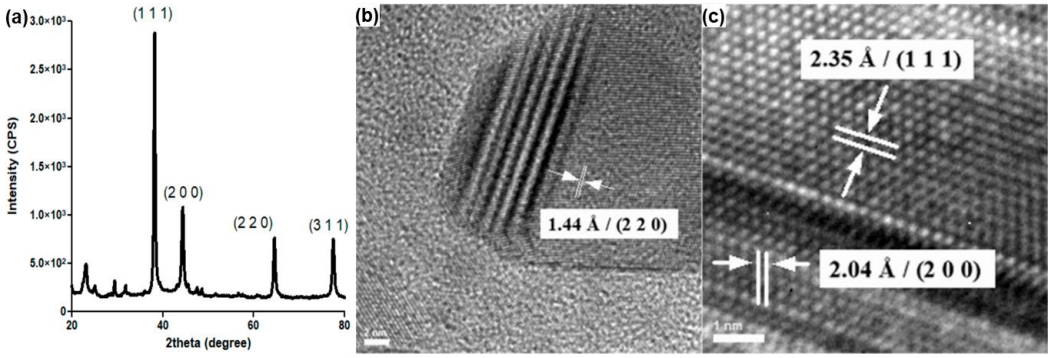

Figure 2.1.1: XRD diffractogram of AgNPs (a); HR-TEM micrographs of AgNPs (b,c)

According to the XRD pattern, metallic silver represented the sole crystalline phase of the obtained powder (Figure 2.1.1a). TEM micrographs confirmed the nanosized dimension of obtained silver particles, with mean particle size of ~49 nm. The previously identified crystalline planes and interplanar distances were evidenced in the HR-TEM micrographs (Figure 2.1.1b,c) and the SAED pattern confirmed the presence of fcc crystalline AgNPs.

To evaluate the effects of laser processing on the PLA/AgNPs material, infrared data of drop-cast sample (corresponding to pristine material) and MAPLE samples were compared. The 400 mJ/cm^2 laser fluence proved the optimal choice for the stoichiometric and efficient transfer of PLA/AgNPs materials. Continuous coatings with irregular surface morphology and ~500 nm thickness were thus obtained, the AgNPs being successfully embedded within the polymer matrix.

The biological response of central venous catheters modified with PLA/AgNPs coatings was evaluated in the presence of EA.hy926 endothelial cells. The nanostructured surfaces did not have cytotoxic effects on normal human-derived eukaryotic cells. The results demonstrated that endothelial cells had a normal metabolism and growth in the presence of PLA/AgNPs coatings, with a characteristic cell cycle profile for adult cells (Figure 2.1.2a). Microbiological results demonstrated that PLA/AgNPs coatings significantly interfered with the development of Gram-positive biofilm, the bacterial population being reduced with more than 2.5 logs (Figure 2.1.2b).

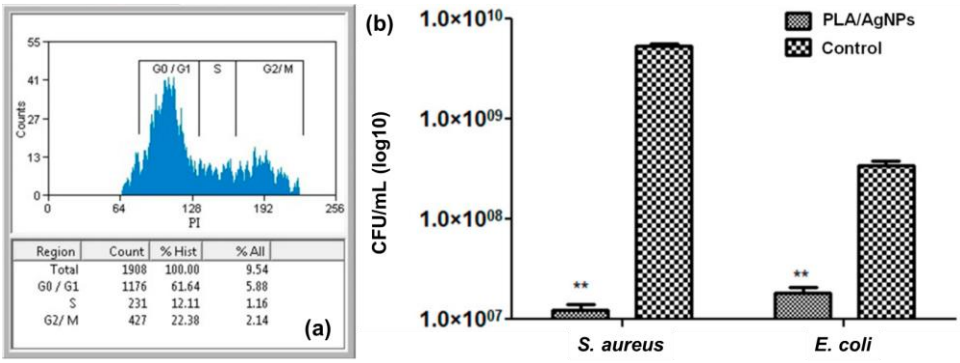

Figure 2.1.2: Cell cycle of endothelial cells after 48h of treatment with PLA/AgNPs coatings (a); Microbial biofilm development of *S. aureus* (left) and *E. coli* (right) strains after 24h of incubation with PLA/AgNPs coatings (b) (** $p \leq 0.01$ sample *vs.* control)

The microbiological results showed the efficiency of PLA/AgNPs coatings to inhibit the first stages of bacterial biofilm formation (attachment, microcolony formation), but also the maturation phase. The proposed nanostructured materials could represent a feasible strategy towards modifying the surface of short-term to mid-term implantable devices.

2.2. Thin films based on polylactide and essential oil – conjugated magnetite nanoparticles

With the aim to revaluate phytochemicals by using nanosized magnetite particles and to optimize the surfaces of biomedical devices by antimicrobial coatings, thin films of polylactic acid (PLA) embedded with iron oxide nanoparticles modified with eucalyptus (*Eucalyptus globulus*) essential oil were herein proposed [23].

IR analysis and thermal studies (Figure 2.2.1a) demonstrated the successful conjugation of *Eucalyptus globulus* (EG) molecules onto Fe_3O_4 particles. The derivatogram corresponding to bare Fe_3O_4 evidenced a total weight loss of 2.81%, which occurred in three steps: (i) exothermic process resulted from $Fe^{2+} \rightarrow Fe^{3+}$ oxidation (100–200°C); (ii) exothermic event occurred due to the thermal degradation of residual organics (300–400°C, weight loss of 1.27%); and (iii) intense

exothermic phenomenon attributed to the isomorphic transformation of iron oxide (mass change of 0.73%) [24,25]. Water chemo-desorption occurred below 100°C (very weak endothermic process), while the elimination of hydroxyl groups was superposed by the first isomorphic transition. Fe_3O_4@EG had a similar thermal pattern, but the process occurred at ~300°C was more intense and accompanied by a mass loss of 1.92% (resulted from the degradation of EG molecules conjugated onto the NPs' surface). A total mass loss of 3.17% was noticed for Fe_3O_4@EG sample.

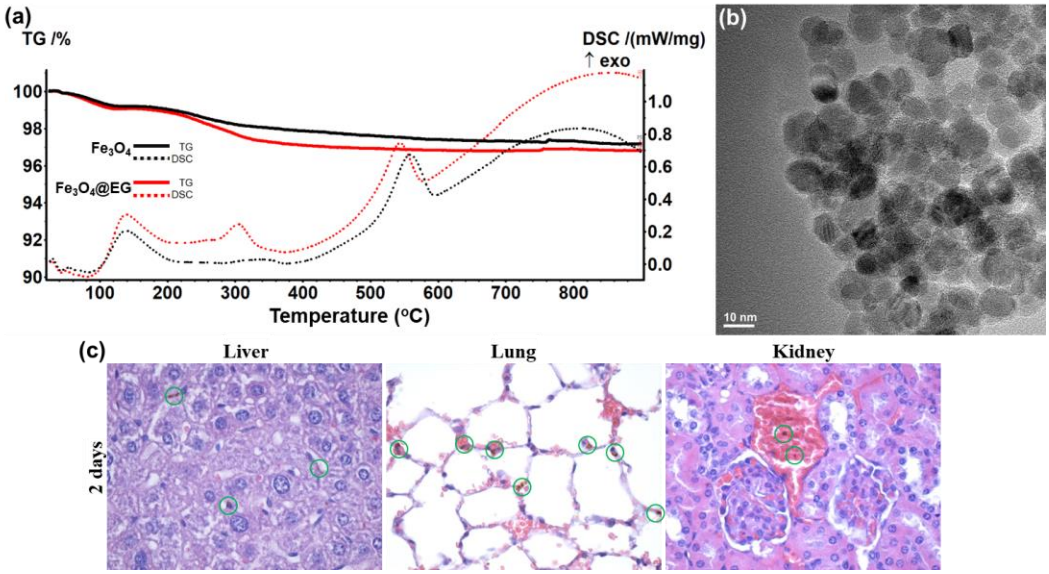

Figure 2.2.1: Thermal analysis of Fe_3O_4 and Fe_3O_4@EG particles (a); TEM micrograph of Fe_3O_4@EG (b); Optical micrographs of hepatic, pulmonary and renal tissues harvested after 2 days of treatment with Fe_3O_4@EG (c)

TEM analysis (Figure 2.2.1b) evidenced the preferential spherical morphology and core/shell structure of Fe_3O_4@EG particles and confirmed their nanosize (7.5 ± 2.5 nm). The SAED pattern confirmed the presence of face-centered spinel structured magnetite. Complementary results evidenced that Fe_3O_4@EG nanoparticles had hydrodynamic diameters between 200.9 and 247 nm, with negative surface charge (-1.7 mV zeta potential).

Preferential tissue retention of Fe_3O_4@EG particles was evidenced after murine systemic administration and histological evaluation. Dark-brown aggregates were noticed within renal capillaries and tissue-specific macrophages of liver and lung, at 2 days after inoculation. Still, no histological alterations were observed in neither of these tissues (Figure 2.2.1c). After 10 days, the liver, lung and kidney were negative for the presence of Fe_3O_4@EG nanoparticles and no ultrastructural modifications or functional alterations were identified. The splenic retention of Fe_3O_4@EG caused a time-dependent hypertrophy of the splenic white pulp.

The homogenous (IR maps) and stoichiometric (IR spectra) transfer of PLA/Fe_3O_4@EG material was evidenced in the case of 300 mJ/cm^2 laser fluence. SEM investigations revealed the uniform and complete coverage of the substrate by the composite material (Figure 2.2.2a), and the uniform distribution of Fe_3O_4@EG aggregates within the PLA matrix (Figure 2.2.2b).

PLA/Fe_3O_4@EG coatings were favorable substrates for the normal development of human mesenchymal stem cells derived from amniotic fluid (AFSCs), since no modification in the metabolic activity of cells was evidenced after 3 days (Figure 2.2.2c). The inhibition of biofilm development by PLA/Fe_3O_4@EG coatings was comparable for all investigated time intervals for both bacteria, with more prominent anti-biofilm efficiency against the Gram-positive strain.

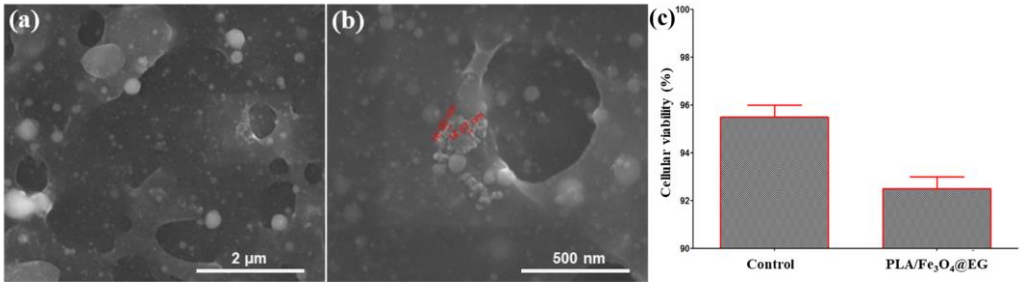

Figure 2.2.2: Plain view SEM micrographs of PLA/Fe_3O_4@EG coatings (a,b);
Viability of mesenchymal stem cells incubated for 72h in the presence of PLA/Fe_3O_4@EG coatings (c)

The biological results evidenced that PLA/Fe_3O_4@EG coatings are highly biocompatible substrates for human-derived cells. The microbiological data indicated that nanostructured PLA/Fe_3O_4@EG materials are suitable candidates for anti-biofilm surface modification of short-term to mid-term implantable biomaterials and devices.

2.3. Thin films based on poly(lactide-co-glycolide) and antibiotic – conjugated magnetite nanoparticles

This study reported the synthesis of nanostructured coatings based on poly(lactic-co-glycolic) acid and magnetite nanoparticles functionalized with a fourth-generation antibiotic (cefepime), PLGA/Fe_3O_4@CEF, as biocompatible and antibacterial coatings for implantable devices [26].

The XRD pattern revealed the presence of broad diffraction maxima at 2θ angles of 30°, 35.80°, 44.10°, 54°, 57.50° and 63.80°. In compliance with the ICDD 19-0629 file and previous results [27,28], the corresponding diffraction planes were specific for the face-centered cubic crystallographic system of magnetite (Figure 2.3.1a). Based on the thermal data corresponding to

Fe_3O_4 and Fe_3O_4@CEF samples, the amount of embedded antibiotic was estimated as 3.53 ± 0.1%. TEM analysis revealed the preferential spherical shape of Fe_3O_4@CEF particles, with mean particle size of ~7 nm (Figure 2.3.1b).

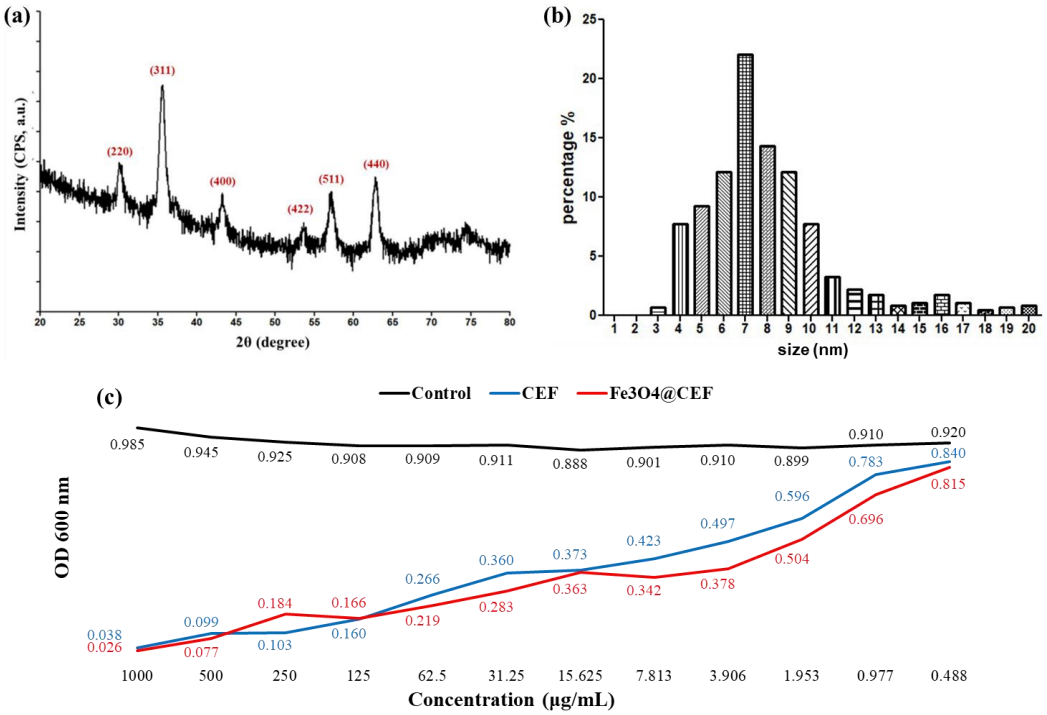

Figure 2.3.1: XRD diffractogram of Fe_3O_4@CEF (a); Particle size histogram of Fe_3O_4@CEF (b); Microbial planktonic development of *S. aureus* after 24h of incubation with Fe_3O_4@CEF and plain CEF (c)

The microbiological evaluation demonstrated the dose-dependent bacteriostatic effects of the obtained nanosystems against microbial growth, with at least similar results as compared with same concentrations of plain CEF solution. *S. aureus* bacterial cells grew slower with an average of ~10% in the presence of Fe_3O_4@CEF at concentrations between 7.8 and 0.9 µg/mL, suggesting the potentiating effects of the obtained nanosystems on the antibiotic's activity.

Infrared maps (Figure 2.3.2, top) resulted by monitoring the stretching vibrations of C=O (~1780 cm^{-1}) and CH_2 (~2950 cm^{-1}) moieties, the absorbance intensity being directly related to colour variations. The abundance of blue-to-green areas was observed in the case of drop-cast sample, due to the non-uniform distribution of PLGA/Fe_3O_4@CEF mixture onto the substrate. In terms of functional groups distribution, a significant improvement was reported for all MAPLE samples, regardless of the laser fluence. The best results were evidenced in the case of 400 mJ/cm^2 laser fluence, which resulted in the efficient and stoichiometric transfer of PLGA/Fe_3O_4@CEF.

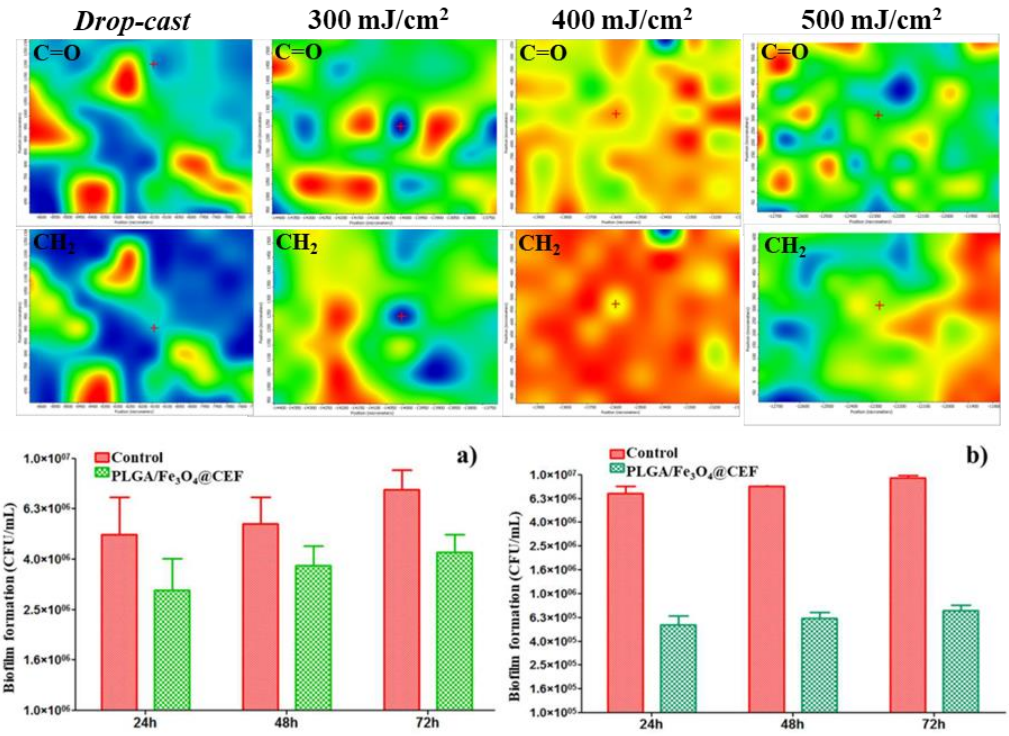

Figure 2.3.2: IR maps of PLGA/Fe_3O_4@CEF drop-cast coating and PLGA/Fe_3O_4@CEF coatings obtained at different laser fluences (top); Microbial biofilm development of *E. coli* (a) and *S. aureus* (b) strains after different incubation periods with PLGA/Fe_3O_4@CEF coatings (down)

The biological results corresponding to the nanostructured coatings were comparable with the control specimens even after 3 days of incubation on AFSCs cultures, the cellular viability variation being lower than 2%. The PLGA/Fe_3O_4@CEF coatings determined the reduced development of bacterial biofilms, regardless of the testing time. (Figure 2.3.2, down). A moderate efficiency of the composite coatings against the development of Gram-negative bacterial biofilm was observed. On the other hand, the nanostructured coatings proved a significant and sustained efficiency against the formation of *S. aureus* biofilm.

Given the sustained strong inhibitory effects exhibited against microbial contamination and colonization, the PLGA/Fe_3O_4@CEF composite coatings proved promising candidates for short to mid-term antimicrobial applications.

2.4. Coatings based on poly(lactide-co-glycolide) microspheres embedded with antibiotic – conjugated magnetite nanoparticles

An interesting and tunable approach for microbial-repellent or microbial-resistant biomedical devices is the development of bioactive coatings that are capable of limiting or even

eliminating the microbial contamination and colonization phenomena. In this respect, composite coatings based on microspheres of PLGA embedded with Fe_3O_4 nanoparticles functionalized with lincomycin (PLGA/Fe_3O_4@LINC) were developed in this study [29].

Fe_3O_4@LINC NPs (mean particle size of ~8 nm, preferential spherical morphology and core/shell structure) were successfully embedded within the PLGA matrix of spheres resulted by microemulsion (Figure 2.4.1.a). When compared to the IR data of Fe_3O_4@LINC nanoparticles, the infrared spectra of PLGA/Fe_3O_4@LINC spheres (Figure 2.4.1b) evidenced the following additional vibrations: symmetric stretching of copolymer-originating carbonyl, overlapped asymmetric stretch of C–O and C–O–C within PVA and PLGA, respectively, and superposed asymmetric stretching –CH_3 and –CH_2– found both within the antibiotic and copolymer (inset).

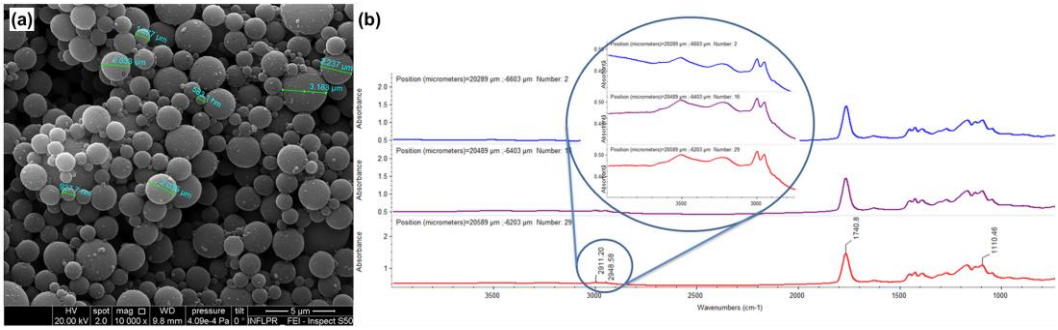

Figura 2.4.1: SEM micrograph of PLGA/Fe_3O_4@LINC spheres (a);
IR spectra of PLGA/Fe_3O_4@LINC spheres and zoomed in region to evidence C–H vibrations (b)

The laser fluence of 400 mJ/cm^2 was experimentally evaluated as optimal for the synthesis of PLGA/Fe_3O_4@LINC composite coatings, resulting in chemical preservation and adequate material transfer.

The ability of PLGA/Fe_3O_4@LINC coatings obtained at different laser fluences to promote cell attachment and sustain cellular growth was quantitatively assessed on human adipose-derived stem cells (hASCs) cultures. At 24h post-seeding, the results revealed good cell viability of hASCs cells for all investigated samples. After 48h, the viability of hASCs cells in contact with PLGA/Fe_3O_4@LINC (500 mJ/cm^2) and Fe_3O_4@LINC nanostructured coatings presented a significant decrease. PLGA/Fe_3O_4@LINC (300 mJ/cm^2) and PLGA/Fe_3O_4@LINC (400 mJ/cm^2) proved a significant up shift of hASCs proliferation potential at 48h post-seeding, showing that both sphere-based nanostructured coatings sustain cell proliferation.

Qualitative biological results (Figure 2.4.2) revealed the higher amount of viable green cells in the case of PLGA/Fe_3O_4@LINC coatings obtained at 300 mJ/cm^2 and 400 mJ/cm^2 laser

fluences. Given the lack of imbalance of live/dead cells ratio corresponding to PLGA/Fe_3O_4@LINC (500 mJ/cm^2) and Fe_3O_4@LINC samples, we concluded that, even if initially these composites allowed cell attachment, they finally failed to sustain cellular proliferation.

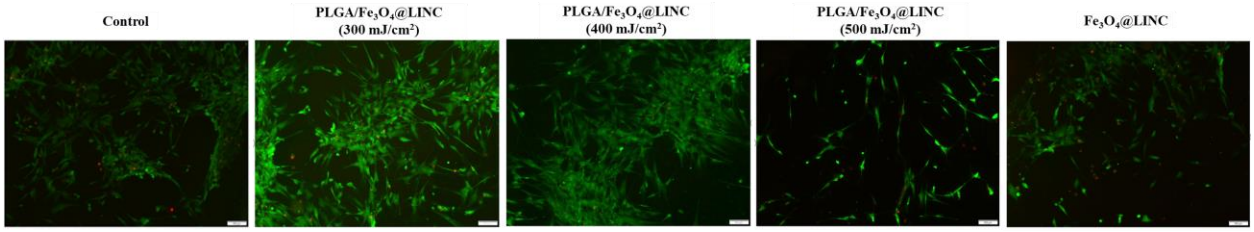

Figure 2.4.2: Viability and proliferation of stem cells grown for 48h in contact with coatings based on PLGA/Fe_3O_4@LINC spheres (300 mJ/cm^2, 400 mJ/cm^2 and 500 mJ/cm^2) and Fe_3O_4@LINC nanoparticles

The fluorescence investigation of hASCs revealed the ability of PLGA/Fe_3O_4@LINC (300 mJ/cm^2 and 400 mJ/cm^2) to support cell adhesion and cytoskeleton development and to promote cellular proliferation, over time (Figure 2.4.3).

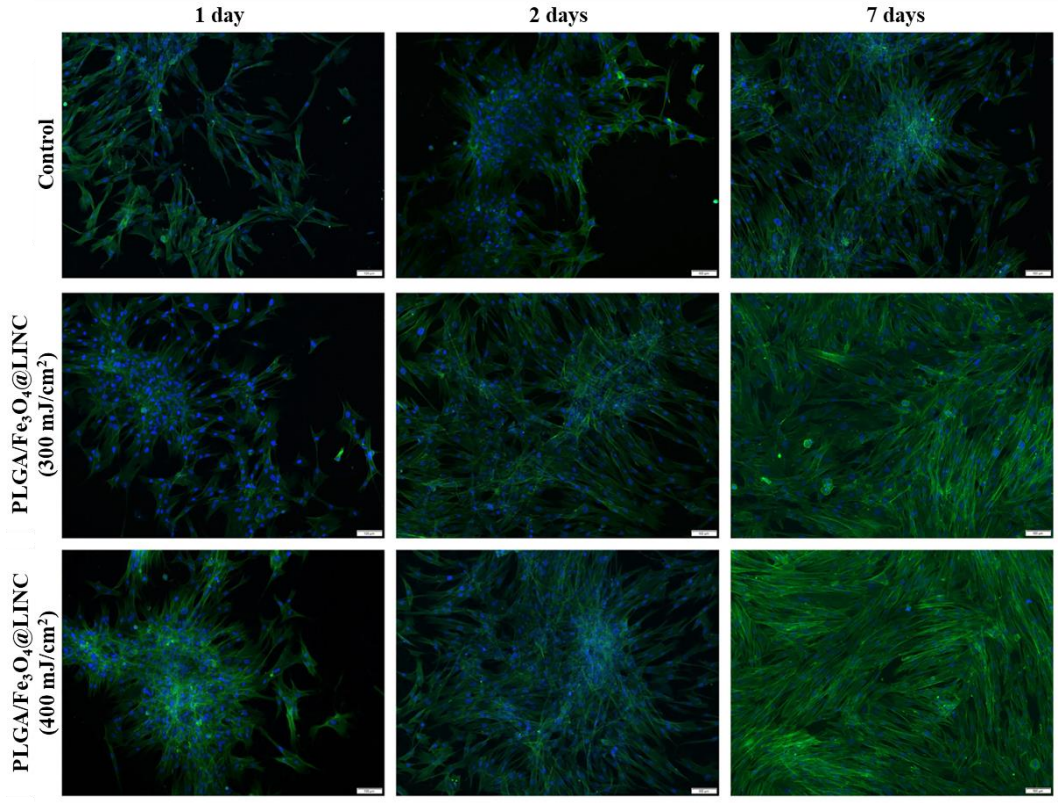

Figure 2.4.3: Morphology of stem cells on PLGA/Fe_3O_4@LINC (300 mJ/cm^2 and 400 mJ/cm^2) coatings after 24h, 48h and 7 days, evidenced by FM showing actin filaments (green) and nuclei (blue)

By gathering the physicochemical results and biological data, we concluded that the laser fluence of 400 mJ/cm^2 represented the optimal choice for the synthesis of nanostructured coatings based on PLGA/Fe_3O_4@LINC spheres for biomedical applications.

The antimicrobial assay proved the increased capacity of composite coatings to inhibit the formation and development of *S. aureus* biofilm, as bacterial bacterial population was reduced with 5 (after 24h) and at least 4 (after 48h) orders of magnitude.

The herein proposed composite coatings based on PLGA spheres embedded with LINC-functionalized magnetite nanoparticles proved suitable biocompatible materials for the antimicrobial treatment of opportunistic complications related to staphylococcal contamination and colonization of implantable devices.

3. Biomimetic nanostructured coatings

3.1. Coatings based on hydroxyapatite, essential oil – conjugated silver nanoparticles and growth factor

To improve the bioactivity of metallic biomaterials and modulate opportunistic contamination and colonization phenomena, nanostructured coatings based on hydroxyapatite, silver nanoparticles conjugated with essential oils (Ag@EOs NPs) and bone morphogenetic protein (BMP4) were proposed in this study.

AgNPs were *in situ* conjugated with sage (*Salvia officinalis* – S) and cinnamon (*Cinnamomum aromaticum* – C) EOs, either by classical (Ag@S and Ag@C) or ultrasound-assisted chemical reduction (Ag@SU and Ag@CU) [30].

Regardless of the type of EO and synthesis conditions, the XRD patterns (Figure 3.1.1) presented intense diffraction maxima at 2θ values of 38.2º, 44.3º and 64.5º. In compliance with PDF No. 00-004-0783 and previous results [31,32], the peaks corresponded to (1 1 1), (2 0 0) and (2 2 0) diffraction planes of face-centered cubic (fcc) crystalline Ag.

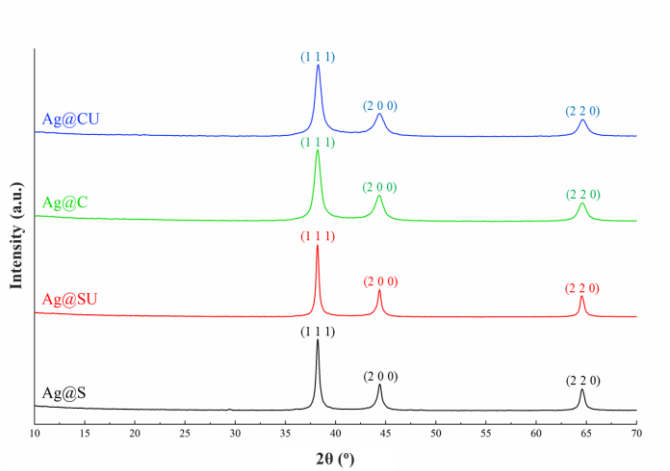

Figure 3.1.1: XRD diffractograms of Ag@EOs

The thermal behavior of Ag-based powdery samples significantly depended on the type of EO used during the synthesis. For AgNPs obtained in the presence of sage EO, a total weight loss of 2.443% and 1.824% was observed for Ag@S and Ag@SU, respectively. These results indicated the predominant metallic character of the particles. In comparison, for AgNPs synthesized in the presence of cinnamon EO, a total weight loss of 48.339% (Ag@C) and 40.625% (Ag@CU) was obtained, which indicated an increased amount of surface-conjugated organic molecules.

TEM micrographs revealed the spherical morphology of all synthesized Ag@EOs NPs, with few rod-shape NPs in the case of Ag@S and Ag@SU samples (related to the significant variations in chemical structure and configuration of sage EO's constituents). The physical particle size was estimated as follows: ~25 nm (Ag@S), ~27 nm (Ag@SU), ~16 nm (Ag@C) and ~19 nm (Ag@CU). HR-TEM analysis evidenced the core/shell structure of all NPs, with uniform organic layers of ~2 nm (Ag@S and Ag@SU) and ~5 nm (Ag@C and Ag@SU) being noticed.

After systemic murine inoculation and subsequent histological examination, the preferential tissue retention of Ag@EO NPs was evidenced. No morphological alterations or ultrastructural modifications were noticed in the brain, myocardium and pancreas tissues, regardless of the testing time (2 and 10 days).

In the case of hepatic and pulmonary tissues, dark-brown aggregates were identified within tissue-specific resident macrophages (hepatic stellate macrophages, and pneumocytes and alveolar macrophages, respectively). Smaller aggregates were observed for Ag@C and Ag@CU samples. Also, the reduced aggregation and increased stability of Ag@EO NPs obtained by sonochemical synthesis led to smaller inorganic deposits after both time intervals.

Ag@EO NPs aggregates were evidenced within the blood vessels of renal fragments, the size and distribution of these aggregates being significantly reduced after 10 days of treatment. No morphological and ultrastructural alterations were identified at this level.

A time-dependent presence of Ag@EO NPs aggregates was observed within the splenic red pulp, accompanied by the substantial hypertrophy of the splenic white pulp (due to NPs-activated overproduction of multilobed nucleated macrophages).

The efficient and stoichiometric transfer of uniform coatings based on hydroxyapatite and silver nanoparticles (HAp/Ag@EOs) was obtained by using the 500 mJ/cm^2 laser fluence. Compact and nanorough coatings, with sub-micron thickness, were thus obtained.

HAp/Ag@EOs coatings exhibited significant and sustained anti-biofilms effects, with an increased inhibition efficiency of microbial biofilms being noticed in the case of HAp/Ag@S and HAp/Ag@C nanostructured coatings.

HAp/Ag@EOs coatings did not interfere with the development of osteoblast cells after 48h, being beneficial substrates for their normal adhesion, spreading and growth (according to FM and SEM studies).

The quantitative evaluation revealed the cytocompatibility of all HAp/Ag@EOs coatings. The addition of bone morphogenetic protein (BMP4) determined a considerable improvement in cellular viability, the viable cells being significantly increased (between 8% and 24%).

In this study, we reported the anti-biofilm efficiency of HAp/Ag@EOs composite coatings, as well as their ability to support the viability, adhesion and normal development of bone cells. Moreover, the addition of osteoinductive protein had a beneficial role on the viability and proliferation of osteoblasts, demonstrating the potential of these nanostructured materials to be used for surface modification of orthopedic and orthodontic implants.

3.2. Coatings based on hydroxyapatite, antibiotic and growth factor

In order to increase the biocompatibility of commercial implant materials by promoting the cell attachment and growth without toxic effects, and to limit the formation of microbial biofilms, composite coatings based on hydroxyapatite (HAp), aminoglycoside antibiotic kanamycin (KAN) and fibroblast growth factor (FGF2) were obtained in this study [33].

In compliance with PDF Card 01-071-5048 and reported literature [34,35], the XRD analysis confirmed the presence of hexagonal HAp as the sole crystalline phase of the powder obtained by chemical synthesis (Figure 3.2.1a). The HAp powdery sample consisted in sharp polyhedral aggregates constituted by individual needle-shaped nanosized particles (Figure 3.2.1b).

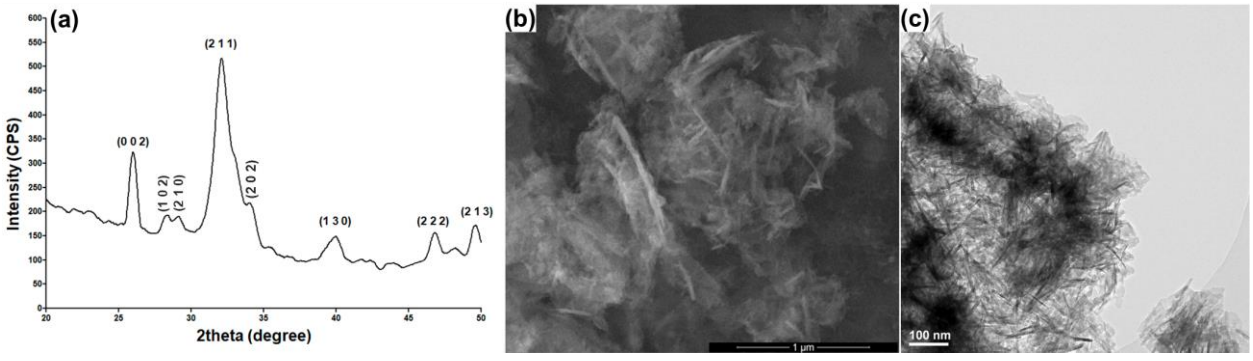

Figure 3.2.1: XRD diffractogram of HAp (a); SEM micrograph of HAp (b); TEM micrograph of HAp (c)

TEM analysis (Figure 3.2.1.c) evidenced the presence of individual nanoparticles with preferential plate and rod morphologies (length below 100 nm and width between 5–25 nm).

In terms of efficient and uniform transfer (IR maps) and preserved chemical integrity (IR spectra), optimal results were evidenced by using the laser fluence of 300 mJ/cm^2. The SEM investigation of HAp/KAN/FGF2 coatings evidenced the unaltered and uniform distribution of composite aggregates onto the substrate. A distinctive rod-shaped morphology of particles could be noticed, but also the presence of an organic outer layer onto the surface of apatite nanoparticles.

The biological behavior of medical graded titanium discs modified with HAp-based coatings was evaluated on MC3T3-E1 preosteoblast cells. The metabolic activity of cells grown on HAp-coated samples was comparable with that of control, with viability variations below 10%. Complementary, the nanostructured surfaces did not induce NO release, its level being maintained close to control values for all samples. Fluorescence micrographs (Figure 3.2.3) showed that MC3T3-E1 grown on HAp-based coatings exhibited good adhesion and uniform spreading onto the substrate. The cells displayed normal morphology and characteristic osteoblast-like phenotype (flattened structure, elongated actin filaments, multiple cytoskeleton extensions, and prominent central nuclei).

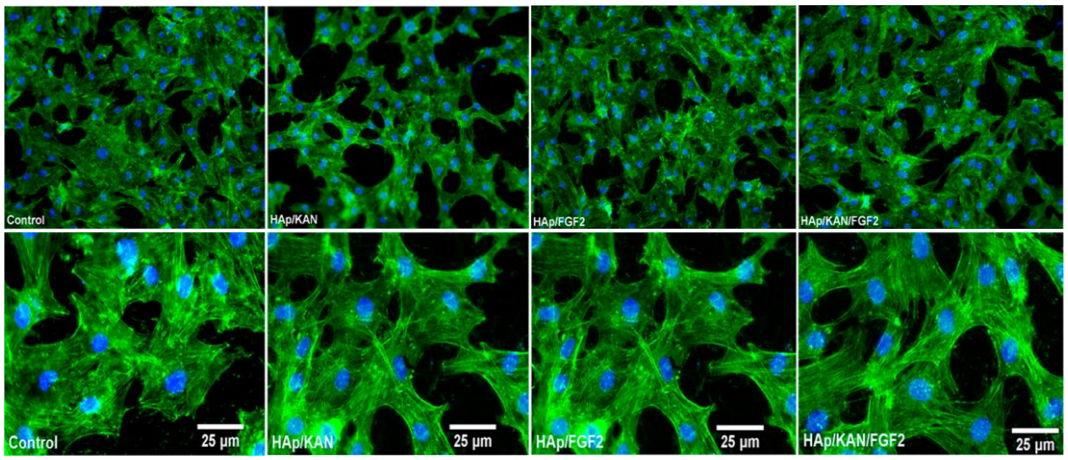

Figure 3.2.2: Morphology of osteoblastic cells on HAp/KAN, HAp/FGF2 and HAp/KAN/FGF2 coatings after 24h, evidenced by FM showing actin filaments (green) and nuclei (blue)

The ability of KAN-embedded coatings to interfere with the formation and development of bacterial biofilms was assessed against opportunistic *S. aureus* and *P. aeruginosa*. A more prominent action was noticed against the Gram-positive strain. The inhibitory effects exhibited by HAp/KAN and HAp/KAN/FGF2 coatings were comparable and more pronounced at 48h, in both situations. Given that the anti-biofilm effect was maintained and even enhanced after 48h,

the stability and preserved biological properties of KAN-embedded nanostructured coatings was evidenced. This period of time is very important when investigating biofilms, since after less than 24h in optimal conditions, biofilms are already mature and dispersion starts.

The MAPLE processed coatings proved prolonged biological activity and sustained anti-biofilm efficiency, representing good candidates for the design of performance-enhanced implants and surfaces, with a significant impact in hard tissue engineering applications.

3.3. Coatings based on polylactide, hydroxyapatite and growth factor

With the aim to improve the bioactivity of metallic implants, we evaluated the ability of MAPLE-processed composite coatings based on polylactide (PLA), hydroxyapatite (HAp) and osteogenic protein (BMP4) to modulate the response of osteoprogenitor cells.

XRD results evidenced the formation of high purity hexagonal-structured HAp. PO_4^{3-} characteristic absorption bands were identified in the IR spectrum of HAp powder: asymmetric and symmetric stretching of P–O, asymmetric deformation of O–P–O. SEM images showed the presence of HAp aggregates, consisting in individual nanosized particles with needle-like morphology (width of ~10 nm, length between 10−100 nm).

In terms of preserved stoichiometry (IR spectra) and transfer efficiency (IR maps), optimal results were found for materials processed with 300 mJ/cm^2 laser fluence. SEM analysis evidenced the formation of uniform and compact coatings, with HAp aggregates being uniformly distributed within the polymer matrix.

The ability of PLA/HAp/BMP4 nanostructured coatings to sustain the adhesion and viability and promote the proliferation of MC3T3-E1 preosteoblast cells was evaluated at 2 and 7 days post-seeding. Qualitative results revealed the increased ability of cells to attach to the surface of PLA/HAp/BMP4 material, as the viable cells covered the substrate evenly and almost completely. Complementary data confirmed the ability of composite coatings to support cell proliferation, the cellular viability being significantly increased after 7 days of culture, compared to that recorded after 2 days. The beneficial interaction of MC3T3-E1 cells with the developed PLA/HAp/BMP4 coatings was also demonstrated by investigating the cellular morphology.

In this study, we reported the increased efficiency of the laser-processed PLA/HAp/BMP4 nanostructured coatings to support the adhesion, viability and proliferation of preosteobleasts, without alterations regarding their normal development.

General conclusions

The main goal of the research activity was to develop bioactive nanostructured platforms for anti-infective therapy and tissue engineering. The performed studies involved the synthesis, optimization and evaluation of new biomaterials, such as: (i) biopolymeric systems (particles and films) designed to potentiate the pharmacological effects of antimicrobial and anti-inflammatory biosubstances; (ii) nanostructured thin films designed to prevent and limit the microbial contamination and colonization of biomedical surfaces; and (iii) nanostructured coatings modified with bioactive molecules designed to modulate infectious processes and regenerative effects of metallic implants.

The original contributions resulted from the first experimental section can be summarized as follows: (i) potentiating the efficacy of polypeptide and aminoglycoside antibiotics by incorporation into P(3HB-3HV)-CS composite microspheres; (ii) modulating the release of bioactive principles and magnetically-activated hyperthermia by means of biosubstance-loaded PLGA-Fe_3O_4 nanostructured microspheres; (iii) developing new platforms with antimicrobial and anti-biofilm activity, such as PLGA-(CS)-Fe_3O_4-IBUP hybrid systems; (iv) modulating the complex cellular interactions at the tissue-to-implant interface, by surface modification of implantable devices with PLGA/IBUP bioactive coatings. The results confirmed the multifunctional ability of P(3HB-3HV)-CS-ATB and PLGA-(CS)-Fe_3O_4-IBUP microspheres and PLGA/IBUP coatings, as they represent promising candidates for the development of effective pharmacotherapeutics for the controlled treatment of infectious and inflammatory pathologies, but also for the performance-enhanced functionality of implantable devices.

The original contributions resulted from the second experimental section include: (i) potentiating the anti-pathogenic effects of phytochemicals and antibiotics by their conjugation to magnetite nanoparticles; (ii) obtaining antimicrobial nanostructured surfaces based on biodegradable polyesters and nanosized particles of silver or magnetite functionalized with bioactive principles; (iii) obtaining antimicrobial hybrid coatings based on biopolymeric microspheres loaded with drug-functionalized nano-magnetite; (iv) modulating the bioactivity and microbial susceptibility of biomedical surfaces by MAPLE coatings; (v) using the MAPLE technique to develop new anti-infective platforms. The experimental results confirmed the potential use of such nanostructured materials as biocompatible coatings for biomedical surfaces, while ensuring the prevention and limitation of microbial contamination and colonization.

Original contributions from the last experimental section can be thus summarized: (i) conjugating natural-derived biomolecules on the surface of nano-silver, using conventional and ultrasound-assisted protocols for reducing metallic salts; (ii) improving the chemical stability of silver nanoparticles and increasing the thermal stability of essential oils through the synthesis of Ag@EOs nanostructures; (iii) modulating the bioactivity and microbial susceptibility of metallic implants by their surface modification with biomimetic and antimicrobial nanostructured coatings; (iv) using the MAPLE technique to successfully embed growth factors within biomimetic coatings. Complementary to previous studies that reported the excellent efficiency of biomaterials modified with growth factors (GFs) by mild chemical protocols, the efficiency of MAPLE processing on the development of GFs-embedded coatings has been demonstrated for the first time. The performed studies revealed the promising use of nanostructured coatings loaded with BMP4 and FGF2 in modulating the bioactivity of metallic implants.

The experimental data resulted from the doctoral research activity highlighted the promising potential of the developed nanostructured biomaterials to be used in revelant biomedical applications, such as controlled anti-infective therapy, management of infectious conditions related to implantable devices and boosted osseointegration of orthopedic and orthodontic metallic implants. Results dissemination in specialized Clarivate-indexed and ISI-indexed interntional journals confirmed and validated the multifunctionality of the nanostructured biomaterials.

Results dissemination

The original contributions obtained during the doctoral studies were disseminated in scientific articles (papers published in international journals) and by attending national and international conferences. Also, *review* papers and book chapters represented an important contribution for the scientific community.

Journal articles:

1. **Gherasim O.**; Grumezescu A.M.; Grumezescu V.; Negut I.; Dumitrescu M.F.; Stan M.S.; Nica I.C.; Holban A.M.; Socol G.; Andronescu E. *Bioactive coatings based on hydroxyapatite, kanamycin, and growth factor for biofilm modulation*. Antibiotics 2021, 10, 160 (IF_{2020} = 4.639)

2. **Gherasim O.**; Grumezescu A.M.; Ficai A.; Grumezescu V.; Holban A.M.; Gălățeanu B.; Hudiță A. *Composite P(3HB-3HV)-CS spheres for enhanced antibiotic efficiency*. Polymers 2021, 13, 989 (IF_{2020} = 4.329)

3. **Gherasim O.**; Popescu-Pelin G.; Florian P.; Icriverzi M.; Roseanu A.; Mitran V.; Cimpean A.; Socol G. *Bioactive ibuprofen-loaded PLGA coatings for multifunctional surface modification of medical devices*. Polymers 2021, 13, 1413 (IF_{2020} = 4.329)

4. **Gherasim O.**; Popescu R.C.; Grumezescu V.; Mogoșanu G.D.; Mogoantă L.; Iordache F.; Holban A.M.; Vasile B.Ș.; Bîrcă A.C.; Oprea O.-C.; Grumezescu A.M.; Andronescu E. *MAPLE coatings embedded with essential oil-conjugated magnetite for anti-biofilm applications*. Materials 2021, 14, 1612 (IF_{2020} = 3.623)

5. **Gherasim O.**; Grumezescu A.M.; Mogoșanu G.D.; Vasile B.Ș.; Bejenaru C.; Bejenaru L.E.; Andronescu E.; Mogoantă L. *Biodistribution of essential oil-conjugated silver nanoparticles*. Romanian Journal of Morphology and Embriology 2020, 61(4), 1099-1109 (IF_{2019} = 1.411)

6. **Gherasim O.**; Grumezescu A.M.; Grumezescu V.; Iordache F.; Vasile B.S.; Holban A.M. *Bioactive surfaces of polylactide and silver nanoparticles for the prevention of microbial contamination*. Materials 2020, 13(3), 768 (IF_{2019} = 3.057)

7. Popescu R.C.; Savu D.I.; Olarescu A.D.; **Gherasim O.**; Banita Ș.; Straticiuc M.; Mirea D.; Andrei R.F.; Trusca R.; Vasile B.Ș.; Socol G.; Andronescu E. *In vitro magnetic targeted delivery of doxorubicin using iron oxide nanoparticles leads to enhanced cell death in glioblastoma*. U.P.B. Scientific Bulletin Series B: Chemistry and Materials Science 2020, 82(4), 73-84

8. Visan A.I.; Popescu-Pelin G.; **Gherasim O.**; Mihailescu A.; Socol M.; Zgura I.; Chiritoiu M.; Sima L.E.; Antohe F.; Ivan L.; Vranceanu D.M.; Cotrut C.M.; Cristescu R.; Socol G. *Long-term evaluation of dip-coated PCL-blend-PEG coatings in simulated conditions*. Polymers 2020, 12, 717 (IF_{2019} = 3.426)

9. **Gherasim O.**; Puiu R.A.; Bîrcă A.C.; Burdușel A.-C.; Grumezescu A.M. *An updated review on silver nanoparticles in biomedicine*. Nanomaterials 2020, 10, 2318 (IF_{2019} = 4.324)

10. Grumezescu V.; **Gherasim O.**; Negut I.; Banita S.; Holban A.M.; Florian P.; Icriverzi M.; Socol G. *Nanomagnetite-embedded PLGA spheres for multipurpose medical applications*. Materials 2019, 12, 2521 (IF_{2018} = 2.972)

11. Grumezescu V.; Negut I.; **Gherasim O.**; Birca A.C.; Grumezescu A.M.; Hudita A.; Galateanu B.; Costache M.; Andronescu E.; Holban A.M. *Antimicrobial applications of MAPLE processed*

coatings based on PLGA and lincomycin functionalized magnetite nanoparticles. Applied Surface Science 2019, 484, 587-599 (IF_{2018} = 5.155)

12. Visan A.I.; Popescu-Pelin G.; **Gherasim O.**; Grumezescu V.; Socol M.; Zgura I.; Florica C.; Popescu R.C.; Savu D.; Holban A.M.; Cristescu R.; Matei C.E.; Socol G. *Laser processed antimicrobial nanocomposite based on polyaniline grafted lignin loaded with gentamicin-functionalized magnetite*. Polymers 2019, 11, 283 (IF_{2018} = 3.164)

13. Teleanu R.I.; **Gherasim O.**; Gherasim T.G.; Grumezescu V.; Grumezescu A.M.; Teleanu D.M. *Nanomaterial-based approaches for neural regeneration*. Pharmaceutics 2019, 11(6), 266 (IF_{2018} = 4.773)

14. Ficai D.; Grumezescu V; **Fufa O.M.**; Popescu R.C.; Holban A.M.; Ficai A.; Grumezescu A.M.; Mogoanta L.; Mogosanu G.D.; Andronescu E. *Antibiofilm coatings based on PLGA and nanostructured cefepime-functionalized magnetite*. Nanomaterials 2018, 8, 633 (IF_{2017} = 3.504)

15. Popescu-Pelin G.; **Fufă O.**; Popescu R.C.; Savu D.; Socol M.; Zgură I.; Holban A.M.; Vasile B.Ş.; Grumezescu V.; Socol G. *Lincomycin–embedded PANI–based coatings for biomedical applications*. Applied Surface Science 2018, 455, 653-666 (IF_{2017} = 4.439)

16. Burdușel A.-C.; **Gherasim O.**; Grumezescu A.M.; Mogoanta L.; Ficai A.; Andronescu E. *Biomedical applications of silver nanoparticles: An up-to-date overview*. Nanomaterials 2018, 681 (IF_{2017} = 3.504)

17. **Fufă O.**; Socol M.; Preda N.; Grigorescu S.; Croitoru S.; Socol G. *MAPLE deposition of PLGA microspheres for medical applications*. Digest Journal of Nanomaterials and Biostructures 2017, 12(1), 73-80 (IF_{2016} = 0.836)

18. Rașoga O.; Sima L.E.; Chirițoiu M.; Popescu-Pelin G.; **Fufă O.**; Grumezescu V.; Socol M.; Stănculescu A.; Zgură I.; Socol G. *Biocomposite coatings based on poly(3-hydroxybutyrate-co-3-hydroxyvalerate)/calcium phosphates obtained by MAPLE for bone tissue engineering*. Applied Surface Science 2017, 417, 204-212 (IF_{2016} = 3.387)

Book chapters:

1. **Gherasim O.** & Grumezescu A.M. *Silver nanoparticles in medicine*. Chapter 3 in: Torchilin V. (Ed.), Handbook of Materials for Nanomedicine: Metal-based and Other Nanomaterials 2020, Jenny Stanford Publishing (Singapore), 111-146 (ISBN 9789814800938)

2. **Gherasim O.**; Grumezescu V.; Socol G.; Ficai A. *Nanoarchitectonics prepared by laser processing and their biomedicinal applications*. Chapter 2 in: Grumezescu A.M. (Ed.), Nanoarchitectonics in Biomedicine 2019, Elsevier (Oxford, UK), 23-53 (ISBN 9780128162002)

3. **Gherasim O.**; Popescu R.C.; Gherasim T.G.; Grumezescu V.; Andronescu E. *Pharmacotherapy and nanotechnology*. Chapter 1 in: Grumezescu A.M. (Ed.), Nanoparticles in Pharmacotherapy 2019, Elsevier (Oxford, UK), 1-21 (ISBN 9780128165041)

4. Bîrca A.; **Gherasim O.**; Grumezescu V.; Grumezescu A.M. *Introduction in thermoplastic and thermosetting polymers*. Chapter 1 in: Grumezescu V. & Grumezescu A.M. (Eds.), Materials for Biomedical Engineering: Thermoset and Thermoplastic Polymers 2019, Elsevier (Oxford, UK), 1-28 (ISBN 9780128168745)

5. Burdusel A.C.; **Gherasim O.**; Grumezescu V.; Grumezescu A.M. *Degradation versus resorption*. Chapter 1 in: Grumezescu V. & Grumezescu A.M. (Eds.), Materials for Biomedical Engineering: Absorbable Polymers 2019, Elsevier (Oxford, UK), 1-18 (ISBN 9780128184158)

6. **Fufă O.**; Vlăsceanu G.M.; Dolete G.; Cabuzu D.; Puiu R.A.; Cîrjă A.; Bogdan N.; Grumezescu A.M. *Nanostructurated composites based on biodegradable polymers and silver nanoparticles*. Chapter 19 in: Thakur V.K.; Thakur M.K.; Kessler M.R. (Eds.), Handbook of Composites from Renewable Materials: Nanocomposites – Science and Fundamentals 2017, Wiley (Massachusetts, USA), 585-621 (ISBN 9781119224365)

7. **Fufă O.**; Popescu R.C.; Gherasim T.G.; Grumezescu A.M.; Andronescu E. *Silver-based nanostructures for cancer therapy*. Chapter 16 in: Ficai A. & Grumezescu A.M. (Eds.), Nanostructures in Therapeutic Medicine Series: Nanostructures for Cancer Therapy 2017, Elsevier (Oxford, UK), 405-428 (ISBN 9780323461443)

8. Popescu R.C.; **Fufa O.**; Apostol A.I.; Popescu D.; Grumezescu A.M.; Andronescu E. *Antimicrobial thin coatings prepared by laser processing*. Chapter 9 in: Ficai A. & Grumezescu A.M. (Eds.), Nanostructures in Therapeutic Medicine Series: Nanostructures for Antimicrobial Therapy 2017, Elsevier (Oxford, UK), 223-236 (ISBN 9780323461528)

9. **Fufă M.O.M.**; Popescu R.C.; Grumezescu A.M.; Holban A.M. *Microorganisms: New trends in environment-friendly and energy-saving water purification*. Chapter 7 in: Grumezescu A.M. (Ed.), Nanotechnology in the Agri-Food Industry: Water Purification 2017, Elsevier (Oxford, UK), 263-288 (ISBN 9780128043004)

10. Popescu R.C.; **Fufă M.O.M.**; Grumezescu A.M.; Holban A.M. *Nanostructurated membranes for the microbiological purification of drinking water*. Chapter 12 in: Grumezescu A.M. (Ed.), Nanotechnology in the Agri-Food Industry: Water Purification 2017, Elsevier (Oxford, UK), 421-446 (ISBN 9780128043004)

Scientific conferences:

1. Florian P.; Icriverzi M.; Grumezescu V.; **Gherasim O.**; Socol G.; Roseanu A. *Ibuprofen and hyaluronic acid – loaded chitosan:PEG coatings for wound healing promotion*. International Symposium on Priorities of Chemistry for a Sustainable Development (PRIOCHEM), October 2021 (ePoster)
2. Duta L.; Chifiriuc M.C.; Grumezescu V.; Stan G.E.; **Gherasim O.**; Popescu-Pelin G.; Craciun V.; Oktar F.N. *Cytocompatible biological-derived hydroxyapatite coatings presenting antimicrobial activity*. European Materials Research Society (E-MRS) Fall Meeting, September 2021 (oral presentation)
3. **Gherasim O.**; Grumezescu A.M.; Grumezescu V.; Negut I.; Stan M.S.; Holban A.M.; Andronescu E. *Bioactive coatings based on hydroxyapatite for biofilm modulation*. E-MRS Spring Meeting, June 2021 (ePoster)
4. Grumezescu V.; **Gherasim O.**; Negut I.; Dorcioman G.; Grumezescu A.M.; Basil H.; Holban A.M. *Fe_3O_4 nanoarchitectures functionalized with eugenol for modulation of virulence and biofilm formation*. E-MRS Spring Meeting, June 2021 (ePoster)
5. Duta L.; Grumezescu V.; Stan G.E.; **Gherasim O.**; Popescu-Pelin G.; Oktar F.N. *Influence of thermal treatments on the morpho-structural and mechanical characteristics of biological-derived HA coatings*. E-MRS Spring Meeting, June 2021 (ePoster)
6. Duta L.; Grumezescu V.; Chifiriuc M.C.; Stan G.E.; **Gherasim O.**; Chioibasu D.; Popescu A.C.; Oktar F.N. *Pulsed laser deposition of cytocompatible biological-derived hydroxyapatite coatings with antimicrobial activity*. E-MRS Spring Meeting, June 2021 (ePoster)
7. Visan A.I.; Popescu-Pelin G.; **Gherasim O.**; Mihailescu A.; Socol M.; Zgura I.; Chiritoiu M.; Sima L.; Antohe F.; Radulescu L.; Vranceanu D.; Cotrut C.; Cristescu R.; Socol G. *Surface functionalization with anticorrosive and antimicrobial biodegradable polymeric implants*. Corrosion and Materials Degradation Web Conference, May 2021 (oral presentation)

8. Popescu R.C.; Olarescu A.D.; **Gherasim O.**; Banita S.; Straticiuc M.; Mirea D.A.; Andrei R.F.; Vasile B.S.; Socol G.; Andronescu E.; Savu D.I. *In vitro magnetic targeted delivery of doxorubicin using iron oxide nanoparticles leads to enhanced cell death*. International Conference on Radiation in Various Fields of Research (RAD), July 2020 (ePoster)

9. Visan A.I.; Popescu-Pelin G.; **Gherasim O.**; Mihailescu A.; Socol M.; Zgura I.; Chiritoiu M.; Sima L.E.; Antohe F.; Ivan L.; Vranceanu D.M.; Cotruț C.M.; Cristescu R.; Socol G. *Dip-coated PCL-blend-PEG coatings degradation comportment in simulated conditions*. National Online Conference of Biophysics (CNB), June 2020 (oral presentation)

10. Icriverzi M.; Florian P.; Moisei M.; **Gherasim O.**; Popescu-Pelin G.; Trif M.; Socol G.; Roșeanu A. *Composite coatings based on PLGA for topical treatment*. PRIOCHEM, November 2019, Bucharest, Romania (poster presentation)

11. Icriverzi M.; Florian P.; Moisei M.; **Gherasim O.**; Popescu-Pelin G.; Trif M.; Socol G.; Roșeanu A. *New composite coatings for topical treatment*. The Annual International Conference of the Romanian Society of Biochemistry and Molecular Biology (RSBMB), September 2019, Iasi, Romania (poster presentation)

12. Vișan A.; Popescu-Pelin G.; **Gherasim O.**; Grumezescu V.; Socol M.; Zgura I.; Florica C.; Popescu R.C.; Savu D.; Holban A.M.; Cristescu R.; Matei C.E.; Socol G. *Electric field-sensitive polymers as controlled Gentamicin sulfate delivery platforms*. E-MRS Spring Meeting, May 2019, Nice, France (oral presentation)

13. Popescu-Pelin G.; **Fufă O.**; Popescu R.C.; Savu D.; Socol M.; Zgură I.; Holban A.M.; Vasile B.Ş.; Grumezescu V.; Socol G. *Synthesis and characterization of Lincomycin–embedded PANI–based coatings*. RSBMB, September 2018, Bucharest, Romania (poster presentation)

14. **Fufă O.** *Acoperiri biocompatibile procesate laser / Laser-processed biocompatible coatings*. Metode și componente electronice. Aplicații și transfer tehnologic / Electronic methods and components. Applications and technology transfer. Research Center for Advanced Materials, Products and Processes (CAMPUS-UPB), May 2018, Bucharest, Romania (oral presentation)

15. **Fufă O.**; Popescu-Pelin G.; Socol M.; Mogoantă L.; Popescu R.C.; Holban A.M.; Socol G.; Crăciun V.; Grumezescu A.M.; Andronescu E. *HAp/AgNPs coatings for titanium-based implants*. International Conference on Advanced Materials (ROCAM), July 2017, Bucharest, Romania (oral presentation)

16. **Fufă O.**; Popescu-Pelin G.; Trușcă R.; Vasile B.Ș.; Socol M.; Zgură I.; Popescu R.C.; Holban A.M.; Grumezescu A.M.; Andronescu E.; Socol G.; Crăciun V. *Bionanostructured CaPs/AgNPs coatings for titanium-based materials.* ROCAM, July 2017, Bucharest, Romania (poster presentation)

17. **Fufă O.**; Stăncălie A.; Miroiu M.; Mihăiescu D.E.; Crăciun V.; Axente E. *Compositional and morphological characterizations of metal implants used in dentistry by spectroscopic techniques*. ROCAM, July 2017, Bucharest, Romania (poster presentation)

18. **Fufă O.**; Vasile B.Ș.; Trușcă R.; Socol M.; Mogoantă L.; Popescu R.C.; Popescu-Pelin G.; Socol G.; Grumezescu A.M.; Andronescu E. *HAp-Ag bionanostructured coatings for titanium implants*. Conference of the Romanian Electron Microscopy Society (CREMS), Mai 2017, Sinaia, Romania (poster presentation)

19. **Fufă O.**; Socol G.; Grumezescu A.M.; Andronescu E.; Trușcă R.; Vasile B.Ș.; Socol M.; Popescu R.C.; Holban A.M. *Biocompatible protective HAp–Ag coatings for titanium implants*. Symposium of the Romanian Chemical Engineering Society (SICHEM), September 2016, Bucharest, Romania (oral presentation)

20. **Fufă O.**; Socol G.; Grumezescu A.M.; Andronescu E.; Socol M.; Popescu R.C.; Holban A.M. *Biocompatible HAp–Ag nanostructured coatings for titanium implants*. International Conference on Photo-Excited Processes and Applications (ICPEPA), September 2016, Brasov, Romania (poster presentation)

Award:

Molecular Systems Design & Engineering (Royal Society on Chemistry) poster award for *Bionanostructured CaPs/AgNPs coatings for titanium-based materials* presentation (International Conference on Advanced Materials – ROCAM2017)

Selected references

1. Tran, T.T. & Tran, P.H. *Nanoconjugation and encapsulation strategies for improving drug delivery and therapeutic efficacy of poorly water-soluble drugs.* Pharmaceutics **2019**, 11(7), 325.
2. Spirescu, V.A.; Chircov, C.; Grumezescu, A.M.; Andronescu, E. *Polymeric nanoparticles for antimicrobial therapies: An up-to-date overview.* Polymers **2021**, 13(5), 724.
3. Huang, H.; Feng, W.; Chen, Y.; Shi, J. *Inorganic nanoparticles in clinical trials and translations.* Nano Today **2020**, 35, 100972.
4. Zheng, K. & Xie, J. *Engineering ultrasmall metal nanoclusters as promising theranostic agents.* Trends in Chemistry **2020**, 2(7), 665-679.

5. Sponchioni, M.; Palmiero, U.C.; Moscatelli, D. *Thermo-responsive polymers: Applications of smart materials in drug delivery and tissue engineering.* Materials Science and Engineering C: Materials for Biological Applications **2019**, 102, 589-605.
6. Mitchell, M.J.; Billingsley, M.M.; Haley, R.M.; Wechsler, M.E.; Peppas, N.A.; Langer, R. *Engineering precision nanoparticles for drug delivery.* Nature Reviews Drug Discovery **2021**, 20(2), 101-124.
7. Begines, B.; Ortiz, T.; Pérez-Aranda, M.; Martínez, G.; Merinero, M.; Argüelles-Arias, F.; Alcudia, A. *Polymeric nanoparticles for drug delivery: Recent developments and future prospects.* Nanomaterials **2020**, 10(7), 1403.
8. Woeppel, K.; Yang, Q.; Cui, X.T. *Recent advances in neural electrode–tissue interfaces.* Current Opinion in Biomedical Engineering **2017**, 4, 21-31.
9. Rupp, F.; Liang, L.; Geis-Gerstorfer, J.; Scheideler, L.; Hüttig, F. *Surface characteristics of dental implants: A review.* Dental Materials **2018**, 34(1), 40-57.
10. Skoog, S.A.; Kumar, G.; Narayan, R.J.; Goering, P.L. *Biological responses to immobilized microscale and nanoscale surface topographies.* Pharmacology and Therapeutics **2018**, 182, 33-55.
11. Graziani, G.; Boi, M.; Bianchi, M. *A review on ionic substitutions in hydroxyapatite thin films: Towards complete biomimetism.* Coatings **2018**, 8(8), 269.
12. Su, Y.; Cockerill, I.; Zheng, Y.; Tang, L.; Qin, Y.X.; Zhu, D. *Biofunctionalization of metallic implants by calcium phosphate coatings.* Bioactive Materials **2019**, 4, 196-206.
13. Rey, C.; Combes, C.; Drouet, C.; Cazalbou, S.; Grossin, D.; Brouillet, F.; Sarda, S. *Surface properties of biomimetic nanocrystalline apatites; applications in biomaterials.* Progress in Crystal Growth and Characterization of Materials **2014**, 60(3-4), 63-73.
14. García-Gareta, E.; Coathup, M.J.; Blunn, G.W. *Osteoinduction of bone grafting materials for bone repair and regeneration.* Bone **2015**, 81, 112-121.
15. Gherasim, O.; Grumezescu, A.M.; Ficai, A.; Grumezescu, V.; Holban, A.M.; Gălățeanu, B.; Hudiță, A. *Composite p(3hb-3hv)-cs spheres for enhanced antibiotic efficiency.* Polymers **2021**, 13(6), 989.
16. Mutlu, G.; Calamak, S.; Ulubayram, K.; Guven, E. *Curcumin-loaded electrospun phbv nanofibers as potential wound-dressing material.* Journal of Drug Delivery Science and Technology **2018**, 43, 185-193.
17. Mazur, K.; Singh, R.; Friedrich, R.P.; Genç, H.; Unterweger, H.; Sałasińska, K.; Bogucki, R.; Kuciel, S.; Cicha, I. *The effect of antibacterial particle incorporation on the mechanical properties, biodegradability, and biocompatibility of pla and phbv composites.* Macromolecular Materials and Engineering **2020**, 305(9), 2000244.
18. Manivasagan, P.; Khan, F.; Hoang, G.; Mondal, S.; Kim, H.; Hoang Minh Doan, V.; Kim, Y.M.; Oh, J. *Thiol chitosan-wrapped gold nanoshells for near-infrared laser-induced photothermal destruction of antibiotic-resistant bacteria.* Carbohydrate Polymers **2019**, 225, 115228.
19. Manivasagan, P.; Hoang, G.; Santha Moorthy, M.; Mondal, S.; Minh Doan, V.H.; Kim, H.; Vy Phan, T.T.; Nguyen, T.P.; Oh, J. *Chitosan/fucoidan multilayer coating of gold nanorods as highly efficient near-infrared photothermal agents for cancer therapy.* Carbohydrate Polymers **2019**, 211, 360-369.
20. Grumezescu, V.; Gherasim, O.; Negut, I.; Banita, S.; Holban, A.M.; Florian, P.; Icriverzi, M.; Socol, G. *Nanomagnetite-embedded plga spheres for multipurpose medical applications.* Materials **2019**, 12(16), 2521.
21. Gherasim, O.; Popescu-Pelin, G.; Florian, P.; Icriverzi, M.; Roseanu, A.; Mitran, V.; Cimpean, A.; Socol, G. *Bioactive ibuprofen-loaded plga coatings for multifunctional surface modification of medical devices.* Polymers **2021**, 13(9), 1413.
22. Gherasim, O.; Grumezescu, A.M.; Grumezescu, V.; Iordache, F.; Vasile, B.S.; Holban, A.M. *Bioactive surfaces of polylactide and silver nanoparticles for the prevention of microbial contamination.* Materials **2020**, 13(3), 768.
23. Gherasim, O.; Popescu, R.C.; Grumezescu, V.; Mogoșanu, G.D.; Mogoantă, L.; Iordache, F.; Holban, A.M.; Vasile, B.Ș.; Bîrcă, A.C.; Oprea, O.C.; Grumezescu, A.M.; Andronescu, E. *Maple coatings embedded with essential oil-conjugated magnetite for anti-biofilm applications.* Materials **2021**, 14(7), 1612.
24. Mohammed, H.B.; Rayyif, S.M.I.; Curutiu, C.; Birca, A.C.; Oprea, O.C.; Grumezescu, A.M.; Ditu, L.M.; Gheorghe, I.; Chifiriuc, M.C.; Mihaescu, G.; Holban, A.M. *Eugenol-functionalized magnetite nanoparticles modulate virulence and persistence in pseudomonas aeruginosa clinical strains.* Molecules **2021**, 26(8), 2189.
25. Lai, C.W.; Low, F.W.; Tai, M.F.; Abdul Hamid, S.B. *Iron oxide nanoparticles decorated oleic acid for high colloidal stability.* Advances in Polymer Technology **2018**, 37(6), 1712-1721.
26. Ficai, D.; Grumezescu, V.; Fufă, O.M.; Popescu, R.C.; Holban, A.M.; Ficai, A.; Grumezescu, A.M.; Mogoanta, L.; Mogosanu, G.D.; Andronescu, E. *Antibiofilm coatings based on plga and nanostructured cefepime-functionalized magnetite.* Nanomaterials **2018**, 8(9), 633.

27. Bruno, A.J.; Correa, J.R.; Peláez-Abellán, E.; Urones-Garrote, E. *A novel method for the functionalization of aminoacids l-glycine, l-glutamic acid and l-arginine on maghemite/magnetite nanoparticles.* Journal of Magnetism and Magnetic Materials **2018**, 456, 87-91.
28. Cursaru, L.M.; Piticescu, R.M.; Dragut, D.V.; Morel, R.; Thébault, C.; Carrière, M.; Joisten, H.; Dieny, B. *One-step soft chemical synthesis of magnetite nanoparticles under inert gas atmosphere. Magnetic properties and in vitro study.* Nanomaterials **2020**, 10(8), 1500.
29. Grumezescu, V.; Negut, I.; Gherasim, O.; Birca, A.C.; Grumezescu, A.M.; Hudita, A.; Galateanu, B.; Costache, M.; Andronescu, E.; Holban, A.M. *Antimicrobial applications of maple processed coatings based on plga and lincomycin functionalized magnetite nanoparticles.* Applied Surface Science **2019**, 484, 587-599.
30. Gherasim, O.; Grumezescu, A.M.; Mogoşanu, G.D.; Vasile, B.Ş.; Bejenaru, C.; Bejenaru, L.E.; Andronescu, E.; Mogoantă, L. *Biodistribution of essential oil-conjugated silver nanoparticles.* Romanian Journal of Morphology and Embryology **2020**, 61(4), 1099-1109.
31. Thiruvengadam, V. & Bansod, A.V. *Characterization of silver nanoparticles synthesized using chemical method and its antibacterial property.* Biointerface Research in Applied Chemistry **2020**, 10(6), 7257-7264.
32. Wang, M.; Li, H.; Li, Y.; Mo, F.; Li, Z.; Chai, R.; Wang, H. *Dispersibility and size control of silver nanoparticles with anti-algal potential based on coupling effects of polyvinylpyrrolidone and sodium tripolyphosphate.* Nanomaterials **2020**, 10(6), 1042.
33. Gherasim, O.; Grumezescu, A.M.; Grumezescu, V.; Negut, I.; Dumitrescu, M.F.; Stan, M.S.; Nica, I.C.; Holban, A.M.; Socol, G.; Andronescu, E. *Bioactive coatings based on hydroxyapatite, kanamycin, and growth factor for biofilm modulation.* Antibiotics **2021**, 10(2), 160.
34. Fang, C.H.; Lin, Y.W.; Lin, F.H.; Sun, J.S.; Chao, Y.H.; Lin, H.Y.; Chang, Z.C. *Biomimetic synthesis of nanocrystalline hydroxyapatite composites: Therapeutic potential and effects on bone regeneration.* International Journal of Molecular Sciences **2019**, 20(23), 6002.
35. Ciocca, L.; Giorgio, L.I.; Sara, R.; Sabrina, G.; Andrea, V.; Annapaola, P.; Alessandro, S.; Barbara, D.; Paolo, M.; Adriano, P.; Giovanna, I.; Achille, T.; Paolo, B. *Nanostructured surface bioactive composite scaffold for filling of bone defects.* Biointerface Research in Applied Chemistry **2020**, 10(2), 5038-5047.